Semiconductors

# Building Blocks for n-Type Organic Electronics: Regiochemically Modulated Inversion of Majority Carrier Sign in Perfluoroarene-Modified Polythiophene Semiconductors**

*Antonio Facchetti, Myung-Han Yoon, Charlotte L. Stern, Howard E. Katz, and Tobin J. Marks**

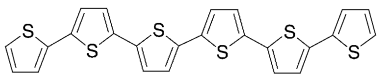

α6T

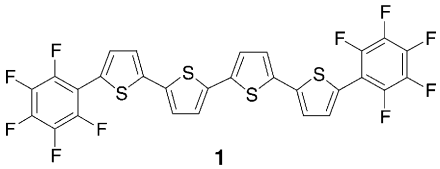

1

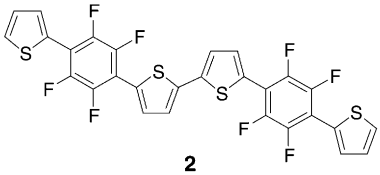

2

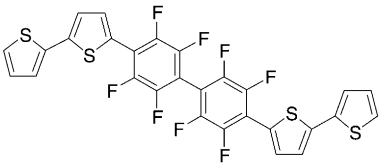

3

Electron-transporting (n-type) organic semiconductors[1] are relatively rare, but of great interest for "plastic electronics" such as thin-film transistors (TFTs), organic light-emitting diodes (OLEDs), and photovoltaics.[2] The most prominent examples of TFT n-type materials have been obtained by modifying known p-type cores with strongly electronegative fluoro/fluoroalkyl substituents. However, despite these advances, those factors underlying fluoro stabilization of the injected electrons are not fully understood, and have often been attributed to the reduction in LUMO energies. Of the known thiophene-based semiconductors, the vast majority[1a,b] exhibit hole-transporting (p-type) TFT activity. However, n-type thiophene-based oligomers and polymers would be extremely useful considering the stability and ready functionalizability of oligothiophene cores.[3]

We report here on the surprising properties of the first fluoroarene-modified thiophene semiconductors **1**–**3**, which can be viewed as p-type **α6T** derivatives drastically reconstituted according to the following criteria: 1) Electronic: electron-deficient perfluoroarene substitution for electron-rich thiophene rings should lower LUMO energies, thus allowing more favorable electron injection. 2) Steric: nonbonded interactions accompanying five→six-membered ring substitution should destabilize ring coplanarity and additionally modulate orbital energies.[4] 3) Regiochemistry: systematic displacement of fluoroarene moieties from the periphery to embedded in the molecular core (**1**→**2**→**3**) can be achieved while preserving rodlike molecular architectures. This is impossible in other classes of molecular semiconductors. 4) Molecular packing: mixing electron-rich and electron-deficient π rings should favor close cofacial π-stacking versus slipped-stacking (herringbone) motifs, as suggested by packing in many 1:1 π-excessive/π-deficient molecular crystals.[5] The net result is a new family of closely packed polythiophene–fluoroarene conductors in which carrier mobility and sign can be drastically modulated by changing the molecular regiochemistry.

Compounds **1**–**3** were prepared in 60–80% yield by $Pd[PPh_3]_4$-catalyzed Stille coupling (Scheme 1), purified by gradient sublimation, and characterized by elemental analysis, mass spectrometry, multinuclear NMR, differential scanning calorimetry, thermogravimetric analysis, and single-crystal X-ray diffraction.[6]

Interestingly, the crystal structures of **1**–**3** (Figure 1)[7] exhibit the common feature of close cofacial packing of electron-rich and electron-deficient subunits, in contrast to all previously reported unsubstituted oligothiophenes (terthiophene to octathiophene) in which a herringbone motif with twist angles of 60–70° between adjacent molecular planes is found. The latter arrangement reduces intermolecular orbital overlap and therefore should increase the barrier to charge transport versus an ideal, π–π overlapped structure. The structures of **1** and **2** reveal substantially planar cores with maximum thiophene–fluoroarene torsional angles between adjacent outer rings of 17.6° and 7.9°, respectively, versus 4.1° for **α6T**.[8] These angles are much smaller than the limiting ≈30° value required for the intramolecular π overlap of an efficient conduction band.[4a,9] Molecules of **1** exhibit an uncommon *syn* conformation between outer pairs of thiophene rings and are stacked in parallel layers along the *b* axis. System **2** packs along *c* in a zig-zag double layer motif, the first layer having an 18.31 Å ($^1/_2c$) repeat distance. Within each layer, the molecular units form slipped π–π stacks. To our

[*] Prof. Dr. T. J. Marks, Dr. A. Facchetti, M.-H. Yoon, Dr. C. L. Stern
Department of Chemistry and
the Materials Research Center
Northwestern University
2145 Sheridan Road, Evanston, IL, 60208-3113 (USA)
Fax: (+1) 847-491-2290
E-mail: tjmarks@casbah.acns.nwu.edu
Dr. H. E. Katz
Bell Laboratories
Lucent Technologies
Murray Hill, NJ 07974 (USA)

[**] We thank DARPA (N00421-98-1187), ONR (N00014-02-1-0909), and the NSF-MRSEC program through the Northwestern Materials Research Center (DMR-0076097) for support of this research.

Supporting information for this article is available on the WWW under http://www.angewandte.org or from the author.

  DOI: 10.1002/ange.200351253 

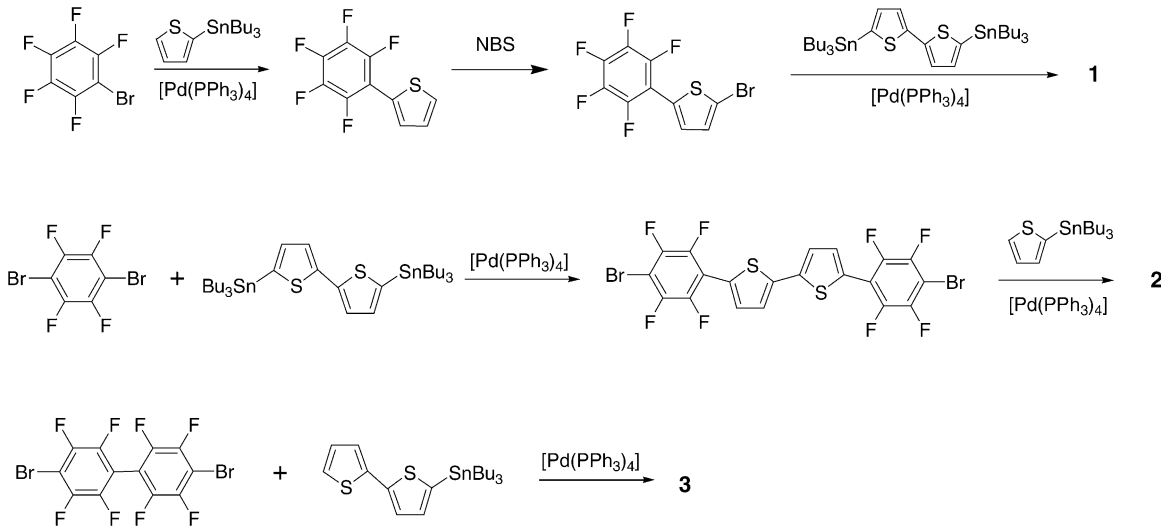


***Scheme 1.*** Synthetic routes to compounds **1**–**3**.

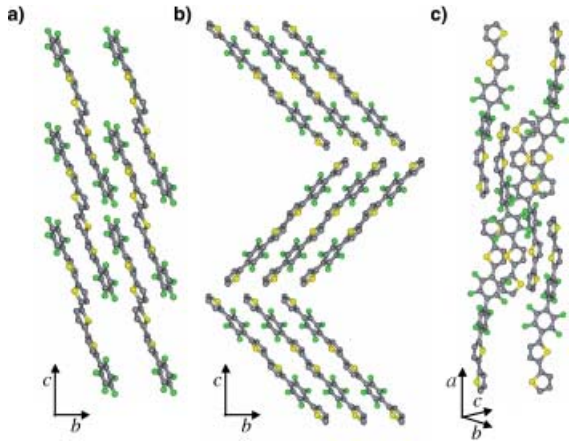


***Figure 1.*** Crystal structures of fluoroarene-thiophene compounds **1** (a), **2** (b), and **3** (c). (C = gray, F = green, S = yellow,).

knowledge, the minimum cofacial π–π distances in **1** (3.20 Å) and **2** (3.37 Å) are the shortest so far reported for thiophene-based oligomers. In contrast, the structure of **3** exhibits a large intramolecular torsional angle (53.9°) between adjacent fluoroarene rings, hence interrupted π conjugation. The packing of **3** is also more complex, with waved layers having the long molecular axes extending along *c*.

Cyclic voltammetry[10] (Table 1) of **α6T** and **1**–**3** as THF solutions or as thin films on Au/glass reveal either two (solution) or one (50 nm films) chemically reversible reductive peaks. Electron affinity increases upon introduction of fluoroaryl rings as evidenced by anodic $E_{1/2}$(THF)/$E_{1/2}$(film) shifts from **α6T** to **1** (+0.20/+0.33 V), **2** (+0.17/+0.31 V), and **3** (+0.16/+0.17 V), respectively. Reversible oxidations are observed in solution for **α6T**, **1**, and **2**, but not for **3**. The film oxidative waves are irreversible as all films dissolve upon cation formation. LUMO energies were calculated directly from reductive $E_{1/2}$ values whereas HOMO energies were estimated from $E_{HOMO} = E_{LUMO} - E_{gap}$(optical).[11] The derived energy level orderings (Figure 2) demonstrate that fluoroarene substitution strongly lowers solution/film HOMO and LUMO energies. However, solution $E_{HOMO}$ values strongly decrease on going from **1**→**2**→**3** ($\Delta E_{HOMO}$(max) = 0.33 eV), whereas film $E_{HOMO}$ and $E_{LUMO}$ values remain in a narrower range ($\Delta E$(max) = 0.16 eV). Therefore, relative stabilization at the molecular level of injected charge should be similar for all of these fluoroarene oligothiophenes, especially for **1** and **2**.

Film microstructure and morphology were investigated by XRD and SEM for 500 nm films vacuum-deposited on 60 °C $Si/SiO_2$ substrates. $\theta$–$2\theta$ X-ray diffraction spectra of **1** and **3** exhibit only one set of Bragg reflections from the same family and a single strong peak, respectively, whereas **2** exhibits two sets of reflections with one being predominant. From the first reflection, interlayer spacings (*d*) of 25.07, 18.38 (14.96 for the second, less intense reflection set), and 5.98 Å are deduced for the films of **1**, **2**, and **3**, respectively, versus 23.3 Å for **α6T**.[12] From the **1**–**3** single-crystal cell parameters,[7] it can be surmised that preferential growth of **1**–**3** crystallites is with the *ab* plane parallel to the substrate surface. Since the molecular long axes are in the *c* direction for **1** and **2** and in the *a* direction for **3**, this corresponds to a preferential orientation of **1** and **2** molecules

***Table 1:*** Solution and Film First Reduction Potentials ($E_{1/2}$),[a] Derived LUMO and HOMO Energies, and Transistor Data[b] for Oligomers α6T[c] and **1**–**3**.

| Oligomers | $E_{1/2}$ [V] | | $E_{LUMO}$ [eV] | | $E_{HOMO}$ (eV) | | μ (type) | *Ion*/*Ioff* |
|---|---|---|---|---|---|---|---|---|
| | THF | Film | THF | Film | THF | Film | | |
| **α6T** | −1.71 | −2.00 | −2.65 | −2.36 | −5.20 | −4.78 | 0.03 (p) | $>10^6$ |
| **1** | −1.51 | −1.67 | −2.85 | −2.69 | −5.48 | −5.27 | 0.08 (n) | $>10^5$ |
| **2** | −1.54 | −1.69 | −2.82 | −2.67 | −5.64 | −5.32 | 0.01 (p) | $10^4$ |
| **3** | −1.55 | −1.83 | −2.81 | −2.53 | −5.81 | −5.40 | $4\times10^{-5}$(p) | $10^2$ |

[a] Versus SCE. Ferrocene used as internal standard. [b] $\mu$ = mobility ($cm^2V^{-1}s^{-1}$), *Ion*/*Ioff* = current on/off ratio. [c] Optimized device. See Ref. [2b].

  

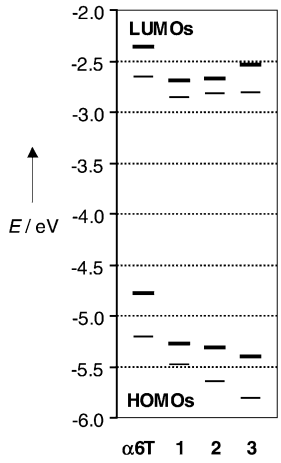


***Figure 2.*** Molecular orbital energy ($E$) level diagram (solution = fine line; film = thick line) for molecules **α6T** and **1**–**3**.

with the long molecular axes along the substrate normal, while **3** molecules orient parallel to the oxide surface. SEM images of **1** and **2**-based films reveal similar morphologies, consisting of highly interconnected crystallites. Smoother and larger grains are found for films of **3**.

Electrical measurements (Table 1) were performed in top source, drain TFT configurations under moderate vacuum ($\approx$20 mTorr). No attempts were made to optimize performance through exhaustive variation in film morphology. Transistor responses are observed only for positive bias for **1**, and for negative bias for **2** and **3** (Figure 3), which means that these materials are n- and p-type semiconductors, respectively. These results combined with the solution/film CV and optical data clearly demonstrate that reduction of the LUMO energy is necessary but not sufficient to promote majority electron transport. The regiochemistry of fluoroarene electron-withdrawing moieties with respect to the π backbone plays a fundamental role in establishing the active

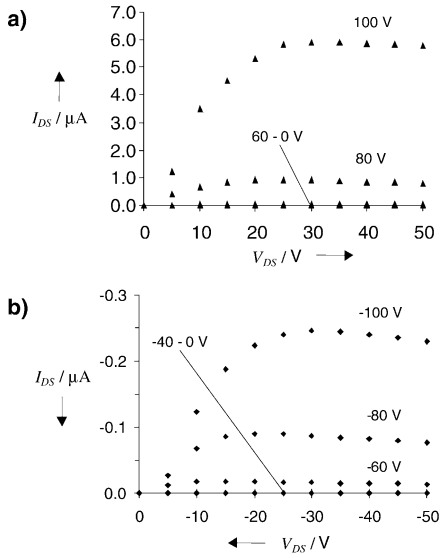


***Figure 3.*** Output characteristics of TFT devices based on films of **1** (a) and **2** (b) at different gate bias.

conducting channel. As shown above, fluoroarene ring displacement along the molecular core dramatically affects packing characteristics and should therefore affect intermolecular orbital overlap.[13] This in turn modulates electronic coupling (bandwidth) between HOMO (for hole transport) and LUMO (for electron transport) levels of adjacent molecules and consequently may greatly affect the corresponding carrier mobilities. Another important factor may be localization of charge in polaronic structures. Maximum charge separation would result in charge localization on the end rings, fluoroarene for **1**, and thiophene for **2** and **3**. The former should preferentially accommodate a negative charge whereas the latter a positive charge. Finally, n- versus p-type transport may be influenced by the superior core screening by the end-fluoroarene groups in **1** against environmental electron traps ($O_2$, $H_2O$), probably at the grain boundaries.[1e]

Since the **1**–**3** film morphologies are similar, mobility trends within the series ($\mu$ ($cm^2V^{-1}s^{-1}$): **1** (0.08) > **2** (0.01) $\gg$ **3** ($4\times10^{-5}$)) can be explained by considering the single-crystal and film microstructural data. Closely π–π stacked planar **1** and **2** are more favorably organized for charge transport in the plane of the substrate than the poorly conjugated structure of **3**. In addition, the highly crystalline, textured films of **1** provide more favorable microstructures for charge transport than less ordered films of **2** having two sets of reflections, which presumably correspond to two crystallite growth orientations. However, both crystal and film microstructures are clearly superior to that of **3**.

In summary, a new polythiophene–fluoroarene conductor family allowing direct scrutiny of regiochemical effects on crystal structure, orbital energies, and charge transport has been synthesized. For the first time, n- and p-type activities have been achieved within the same series by manipulating relative building-block connectivity. Proper LUMO energy and molecular regiochemistry results in n-type activity only for **1**, with $\mu = 0.08\ cm^2V^{-1}s^{-1}$—the highest mobility yet reported in the thiophene series. Enclosing the fluoroaryl fragments within the thiophene(s) core results in more (**2**) or less (**3**) efficient p-type structures, depending on the corresponding film microstructure and molecular self-organization. This study therefore provides fundamental insight into the improved design and understanding of fluoroaromatic n-type semiconductors.

Received: February 24, 2003
Revised: May 16, 2003 [Z51253]

**Keywords:** conducting materials · electron transport · fluorine · semiconductors · thiophene oligomers

[1] a) A. Facchetti, M. Mushrush, H. E. Katz, T. J. Marks, *Adv. Mater.* **2003**, *15*, 33; b) T. M. Pappenfus, R. J. Chesterfield, C. D. Frisbie, K. R. Mann, J. Casado, J. D. Raff, L. L. Miller, *J. Am. Chem. Soc.* **2002**, *124*, 4184; c) A. Yassar, F. Demanze, A. Jaafari, M. El Idrissi, C. Coupry, *Adv. Funct. Mater.* **2002**, *12*, 699; d) P. R. L. Malenfant, C. D. Dimitrakopoulos, J. D. Gelorme, L. L. Kosbar, T. O. Graham, A. Curioni, W. Andreoni, *Appl. Phys. Lett.* **2002**, *80*, 2517; e) B. Crone, A. Dodabalapur, Y. Y. Lin, R. W. Filas, Z. Bao, A. LaDuca, R. Sarpeshkar, H. E. Katz,

  

W. Li, *Nature* **2000**, *403*, 521; f) So. B. Heidenhain, Y. Sakamoto, T. Suzuki, A. Miura, H. Fujikawa, T. Mori, S. Tokito, Y. Taga, *J. Am. Chem. Soc.* **2000**, *122*, 10240; g) A. Facchetti, Y. Deng, A. Wang, Y. Koide, H. Sirringhaus, T. J. Marks, R. H. Friend, *Angew. Chem.* **2000**, *112*, 4721; *Angew. Chem. Int. Ed.* **2000**, *39*, 4547; h) M. L. Renak, G. P. Bartholomew, S. Wang, P. J. Ricatto, R. J. Lachicotte, G. C. Bazan, *J. Am. Chem. Soc.* **1999**, *121*, 7787; i) Z. Bao, A. J. Lovinger, J. Brown, *J. Am. Chem. Soc.* **1998**, *120*, 207.

[2] a) C. D. Dimitrakopoulos, P. R. L. Malenfant, *Adv. Mater.* **2002**, *14*, 99; b) F. Würthner, *Angew. Chem.* **2001**, *113*, 1069; *Angew. Chem. Int. Ed.* **2001**, *40*, 1037.

[3] a) *Handbook of Organic Conducting Molecules and Polymers, Vols. 1–4* (Ed.: H. S. Nalwa), Wiley, Chichester, **1997**.

[4] a) *Handbook of Conducting Polymers* (Eds.: T. A. Skotheim, R. L. Elsenbaumer, J. R. Reynolds), Marcel Dekker, New York, **1998**; b) K. Meerholz, J. Heinze, *Electrochim. Acta* **1996**, *41*, 1854.

[5] a) Online Cambridge Crystallographic Database; b) *Crystal Structure Determination* (Ed.: M. Warner), Teubner, Stuttgart, **1996**, and reference therein.

[6] The Supporting Information includes: Experimental details, TGA and CV plots, single crystal and film XRD data, SEM micrographs and *I–V* plot for compound **3**, cyclic voltammograms, and details of device fabrication.

[7] Single crystals of **1**–**3** were grown by either vacuum sublimation or cooling of saturated solutions. All measurements were made on a Bruker SMART CCD diffractometer with graphite monochromated $Mo_{K\alpha}$ (0.71073 Å) radiation. The data were collected at a temperature of 153(2) K and the structures were solved by direct methods and expanded using Fourier techniques using SHELXTL. All non-hydrogen atoms were refined anisotropically. Hydrogen atoms were included in idealized positions and not refined. Intensities were corrected for absorption. **1**. Crystal size: $0.160\times0.054\times0.032$ mm. Triclinic, $P\bar{1}$, $Z=1$. Cell dimensions: $a=6.3854(15)$ Å; $b=7.6862(18)$ Å; $c=12.502(3)$ Å; $\alpha=89.412(4)°$; $\beta=78.660(4)°$; $\gamma=80.760(4)°$. $V=593.7(2)$ Å$^3$, $2\theta_{max}=56.82$, $\rho_{calcd}=1.853\,g\,cm^{-3}$. Of 5530 reflections, 2751 were independent ($R_{int}=0.064$), 190 parameters, $R1=0.066$ (for reflections with $I>2\sigma(I)$), $wR2=0.160$ (for all reflections). **2**. Crystal size: $0.600\times0.136\times0.044$ mm. Monoclinic, $P2(1)/n$, $Z=2$. Cell dimensions: $a=6.258(2)$ Å; $b=5.0431(14)$ Å; $c=36.618(11)$ Å; $\alpha=90.00°$; $\beta=90.71(3)°$ $\gamma=90.00°$. $V=1155.6(6)$ Å$^3$, $2\theta_{max}=57.64$, $\rho_{calcd}=1.801\,g\,cm^{-3}$. Of 10121 reflections, 2835 were independent ($R_{int}=0.073$), 181 parameters, $R1=0.086$ (for reflections with $I>2\sigma(I)$), $wR2=0.272$ (for all reflections). **3**. Crystal size: $0.512\times0.076\times0.062$ mm. Orthorhombic, *Pbcn*, $Z=4$. Cell dimensions: $a=25.754(5)$ Å; $b=7.625(2)$ Å; $c=11.842(2)$ Å; $\alpha=90.00°$; $\beta=90.00°$; $\gamma=90.00°$. $V=2325.5(9)$ Å$^3$, $2\theta_{max}=57.92$, $\rho_{calcd}=1.790\,g\,cm^{-3}$. Of 20218 reflections, 2931 were independent ($R_{int}=0.047$), 188 parameters, $R1=0.048$ (for reflections with $I>2\sigma(I)$), $wR2=0.124$ (for all reflections). CCDC 207396 (**1**), CCDC 207397 (**2**), CCDC 207398 (**3**) contain the supplementary crystallographic data for this paper. These data can be obtained free of charge via www.ccdc.cam.ac.uk/conts/retrieving.html (or from the Cambridge Crystallographic Data Centre, 12, Union Road, Cambridge CB21EZ, UK; fax: (+44) 1223-336-033; or deposit@ccdc.cam.ac.uk).

[8] D. Fichou, *J. Mater. Chem.* **2000**, *10*, 571.

[9] a) R. D. McCullough, *Adv. Mater.* **1998**, *10*, 93; b) J.-L. Brédas, *J. Chem. Phys.* **1985**, *82*, 3809.

[10] Measurements performed in $O_2$- and moisture-free $n$-$Bu_4NPF_6$/THF in a one-compartment cell with a C disk working electrode, a bare Ag reference, and Pt wire counter electrodes.

[11] A. J. Bard, L. R. Faulkner, *Electrochemical Methods—Fundamentals and Applications*, Wiley, New York, **1984**. Note that **α6T**, **1**, and **2** $E_{HOMO}$ values calculated from reversible oxidation potentials (−5.34, −5.55, and −5.64 eV, respectively) and optical $E_{gap}$ data (see Table 1) are in excellent agreement. Solution (THF) optical $E_{gap}$ (eV): 3.00 (**3**), 2.82 (**2**), 2.63 (**1**), 2.55 (**α6T**). Film optical $E_{gap}$ (eV): 2.87 (**3**), 2.65 (**2**), 2.58 (**1**), 2.42 (**α6T**).

[12] A. J. Lovinger, L. J. Rothberg, *J. Mater. Res.* **1996**, *11*, 1581.

[13] J. Cornil, D. Beljonne, J.-P. Calbet, J.-L. Brédas, *Adv. Mater.* **2001**, *13*, 1053.

  